Gas-Phase Nazarov Cyclization of Protonated 2-Methoxy and 2-Hydroxychalcone: An Example of Intramolecular Proton-Transport Catalysis

Mathai George,[a] Valarkottu S. Sebastian,[a] Putluri Nagi Reddy,[b] Ragampeta Srinivas,[b] Daryl Giblin,[c,] and Michael L. Gross[c]

[a] Department of Chemistry, Sacred Heart College, Thevara, Cochin, Kerala, India
[b] National center for Mass Spectrometry, IICT, Hyderabad, India
[c] Department of Chemistry, Washington University in St. Louis, St. Louis, Missouri, USA

Upon CA, ESI generated $[M + H]^+$ ions of chalcone (benzalacetophenone) and 3-phenylindanone both undergo losses of H_2O, CO, and the elements of benzene. CA of the $[M + H]^+$ ions of 2-methoxy and 2-hydroxychalcone, however, prompts instead a dominant loss of ketene. In addition, CA of the $[M + H]^+$ ions of 2-methoxy-β-methylchalcone produces an analogous loss of methylketene instead. Furthermore, the $[M + D]^+$ ion of 2-methoxychalcone upon CA eliminates only unlabeled ketene, and the resultant product, the $[M + D - \text{ketene}]^+$ ion, yields only the benzyl-d_1 cation upon CA. We propose that the 2-methoxy and 2-hydroxy (*ortho*) substituents facilitate a Nazarov cyclization to the corresponding protonated 3-arylindanones by mediating a critical proton transfer. The resultant protonated indanones then undergo a second proton transport catalysis facilitated by the same *ortho* substituents producing intermediates that eliminate ketene to yield 2-methoxy- or 2-hydroxyphenyl-phenyl-methylcarbocations, respectively. The basicity of the *ortho* substituent is important; for example, replacement of the *ortho* function with a chloro substituent does not provide an efficient catalyst for the proton transports. The Nazarov cyclization must compete with an alternate cyclization, driven by the protonated carbonyl group of the chalcone that results in losses of H_2O and CO. The assisted proton transfer mediated by the *ortho* substituent shifts the competition in favor of the Nazarov cyclization. The proposed mechanisms for cyclization and fragmentation are supported by high-mass resolving power data, tandem mass spectra, deuterium labeling, and molecular orbital calculations. (J Am Soc Mass Spectrom 2009, 20, 805–818) © 2009 American Society for Mass Spectrometry

The acid-catalyzed cyclization of divinyl ketones to yield cyclopentenones is known as Nazarov cyclization, a reaction that was recently reviewed [1, 2]. Bronsted acids, superacids, and Lewis acids are usually needed to promote the cyclizations in solution. The mechanism involves conrotatory electrocyclic ring closure of a protonated divinyl ketone followed by deprotonation and double-bond reorganization [2]. A general and efficient method for the synthesis of biologically active 3-aryl-indanones is the Nazarov cyclization of substituted chalcones [3–6]. A variety of indanone derivatives can be synthesized by the microwave-assisted Nazarov cyclization of chalcones in trifluoroacetic acid (TFA) solution [5]. In addition, further motivation comes from the antimicrobial activity of substituted chalcones, which was evaluated recently [7].

Address reprint requests to Dr. M. George, Department of Chemistry, Sacred Heart College, Thevera, Cochin, Kerala 682013, India. E-mail: georgem_mathai@yahoo.co.in and Dr. D. Giblin, Department of Chemistry, Washington University, 1 Brookings Drive, Campus Box 1134, St. Louis, MO 63130, U.S.A. E-mail: giblin@wustl.edu

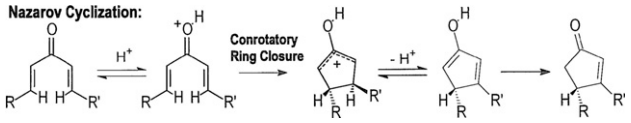

Characterization of these materials has attracted the attention of mass spectrometrists since the early 1960s [8]. The formation and structures of the $[M - H]^+$ ion and $[M - H - CO]^+$ ions from the $M^{+\cdot}$, were one focus [9–14], including an ion-structure study with an ion-trap mass spectrometer [15]. Recently, the mechanisms for elimination of C_6H_6 and CO from the atmospheric pressure chemical ionization (APCI)-generated $[M + H]^+$ ions of chalcones were established [16]. Three important product ions observed in the CAD mass spectrum of protonated chalcone arise from losses of H_2O, CO, and C_6H_6. Studies of the substituted chalcones show that both of the phenyl rings are eliminated as the neutral arenes.

We took a different tack and describe here the possibility of conducting the Nazarov cyclization of chalcones in the gas phase by using a mass spectrome-

1044-0305/09/$32.00
doi:10.1016/j.jasms.2008.12.017

Published online December 31, 2008
Received October 16, 2008
Revised December 18, 2008
Accepted December 18, 2008

ter as both reactor and detector. Investigations of gas-phase reactions conducted using advanced experimental techniques in mass spectrometry and supported by theoretical calculations provide a means for understanding energetics and intrinsic mechanisms of reactions at the molecular level [17, 18]. Ionization methods such as CI and ESI are effective for protonating organic molecules while MS/MS and molecular modeling are widely used for the elucidation of gas-phase structures and fragmentation mechanisms. Proton-induced, gas-phase rearrangements may closely parallel those in solution as demonstrated by mass spectrometric studies; the acid-catalyzed Claisen rearrangement being a classic example [19]. A more recent example is the rearrangement of protonated 2-[*N*-benzoyloxyphenyl] benzamide both in the gas phase and in solution [20]. Another motivation for our study relies on evidence from both experiment and theory that high-energy 1,3-H shifts take place in the gas phase when catalyzed by a base, a process called proton transport catalysis [21–24]. The catalysis of the gaseous acetone radical cation enolization by benzonitrile [25, 26] and methanol [27] as well as the isomerizations of isoformyl/formyl cations by various neutrals [22] of ionized acetaldehyde by methanol are such examples [28].

We expected that ESI or CI methods protonate chalcones at the carbonyl oxygen, affording species that could potentially undergo Nazarov type cyclizations in the gas phase. An important step in the solution Nazarov cyclization is deprotonation. A substituent such as OCH_3 or OH at the *ortho* position may be sufficiently basic to cause deprotonation or otherwise assist in proton transport. Given that the OCH_3 and OH groups are capable of catalyzing proton migrations in the gas phase [27, 28], we chose to synthesize the following chalcones (substituted benzalacetophenones): chalcone (**1**), isomeric methoxy chalcones (**2** and **5**), isomeric hydroxy chalcones (**4** and **6**), 2-methoxy-β-methyl-chalcone (2-methoxybenzal-propiophenone) (**3**), and 2-chloro-chalcone (**7**) for this investigation. In addition, benzhydrols **8**, **9**, and **10** were synthesized and used to generate reference ions.

Experimental

Materials

Chalcones **1** to **7** were synthesized by standard procedures [9, 29, 30] with focus on various substituents at the 2- and 4-position of the **'a'** ring. The benzhydrols used for generating product ions for comparison were synthesized by procedures already reported [31]. Purity of the samples was checked by TLC, and the structures confirmed by NMR, IR and mass spectra (Supplemental Materials, which can be found in the electronic version of this article). 3-Phenyl-indanone was purchased form Aldrich Chemical Co. (Milwaukee, WI).

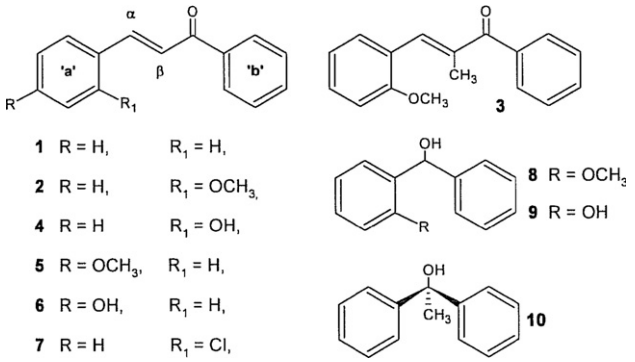

Mass Spectrometry

Instrumental methods. Formation of $[M + H]^+$ ions was achieved by protonation of the chalcones by CI (chemical ionization) and ESI (electrospray ionization) methods. The $[M + H]^+$ ions were analyzed by MS and tandem MS/MS and MS^3 methods by using MI (metastable ion) or CA (collisional activation) under either low-energy (<100 eV, laboratory) or high-energy (4 keV, laboratory) conditions.

The CI experiments, both MS and high-energy CA MS/MS, were conducted on a VG ZAB-T four-sector mass spectrometer (Manchester, UK) of BEBE design [32]. MS1 was a standard high-resolving power, double-focusing mass spectrometer (ZAB) of reverse geometry. MS2 possessed a prototype Mattauch-Herzog-type design, incorporating a standard magnet and a planar electrostatic analyzer having an inhomogeneous electric field, a single-point, and an array detector. Samples were introduced by evaporation from a direct-insertion probe; and ions formed were accelerated to 8 keV. The dissociation of the precursor ion (MI or CAD) was studied in the third field-free region. For CA, sufficient helium gas was added to the collision cell, which was floated at 4 kV, to decrease the main beam intensity by 30% for CAD experiments. Both MS1 and MS2 were operated at a mass resolving power of 1000. Typically 10 to 20 scans were signal averaged for each spectrum. Data acquisition and workup were accomplished by using a VAX 3100 workstation working with OPUS software (VG, Manchester, UK).

The ESI-generated ions were produced from samples dissolved in 1:1 mixture of acetonitrile and water (10–20 μg/mL) and introduced by direct infusion at a flow rate of 10 μL/min for both MS and low-energy tandem MS analyses.

Some ESI and MS/MS experiments were conducted by using a Micromass Q-TOF-Ultima GLOBAL mass spectrometer (Manchester, UK) operated in the positive-ion mode. The needle voltage was 3 kV, and the cone voltage was 90 V. The temperatures of the source block and desolvation region were 90 and 150 °C, respectively. All parameters (i.e., aperture to the TOF, transport voltage, offset voltages) were optimized to achieve maximum sensitivity and a mass resolving

Table 1. CAD mass spectra of ESI-produced $[M + H]^+$ ions (quadrupole ion trap)

Compound	Fragment ions: *m/z* (abundance)						
	$-H_2O$	$-CO$	$-C_6H_6$	$-C_6H_5R$	−Ketene (−Methyl Ketene*)	Benzoyl *m/z* 105	*m/z* 103
Chalcone (**1**)	191 (13)	181 (14)	131 (100)		ND	(10)	(4)
3-Pphenylindanone	191 (2)	181 (1)	131 (100)		ND	ND	(6)
2-Methoxychacone (**2**)	ND	ND	ND	ND	197 (100)	(2)	ND
2-Methoxy-β-methylchalcone (**3**)	235 (32)	ND	ND	ND	*197 (100)	ND	ND
2-Hydroxychalcone (**4**)	ND	ND	ND	ND	183 (100)	(80)	ND
4-Methoxychalcone (**5**)	221 (28)	211 (24)	161 (100)	131 (33)	ND	(55)	(3)
4-Hydroxychalcone (**6**)	207 (28)	197 (25)	147 (100)	131 (22)	ND	(41)	(2)
2-Chlorochalcone (**7**)	225 (14)	215 (9)	165 (100)	131 (26)	201 (2)	(4)	(8)

power of 15,000 (full width at half maximum). The CAD experiments were carried out by mass selecting the precursor ion by using the quadruple analyzer, and the product ions were obtained by using the time-of-flight analyzer operated at a mass resolving power of 15,000 ('w' mode). Collision voltages for fragmenting the ions were in the range of 7 to 10 V with Ar as collision gas. Accurate masses of the product ions were determined by using the precursor ion as the internal standard.

Some ESI MS and low-energy MS/MS and tandem MS^3 experiments were performed by using a Thermo Finnigan LCQ Advantage or a Thermo Finnigan LCQ Classic 3D ion-trap mass spectrometers (San Jose, CA).

Isotopic labeling. To track fragmentation pathways, $[M + D]^+$ ions were generated by using CD_4 CI and were analyzed by high-energy CA and MI methods. In addition, $[M + D]^+$ ions were generated by ESI from 1:1 D_2O/acetonitrile mixture, introduced by direct infusion (10 μL/min) and analyzed by CA MS/MS and MS^3 on the LCQ Classic ion trap.

Theoretical Calculations

Owing to the large size of chalcones, many of the initial scans of the potential energy surfaces were performed by using the PM3 [33, 34] semi-empirical algorithm, where PM3 was part of the Spartan '02 for Linux package (Wave Function, Inc. Irvine, CA). Further characterization was by density functional theory (DFT), which requires less computational overhead than do formal ab initio methods and yet incorporates dynamic correlation, has little spin contamination [35–37], and usually performs adequately giving proper geometries, energies, and frequencies [38]. DFT was part of the Gaussian 98/03 suite (Gaussian, Inc. Wallingford, CT) [39, 40]. Minima and transition states were optimized at the level B3LYP/6-31G(d, p) and confirmed by vibration frequency analysis. Connections of transition states to minima were analyzed by combination of inspection, projection along normal reaction coordinates, or reaction-paths calculations as needed; also discovered by the latter method were complexes (e.g., ion-dipole). Single-point energies were calculated at B3LYP/6-311+G(2d,p)//B3LYP-6-31G(d,p) level and scaled thermal-energy corrections for standard conditions were applied [41]. All calculated enthalpies are reported as relative to the initial protonated chalcone in kJ/mol.

Experimental Results and Discussion

*Chalcone (**1**)*

There are three major fragment ions in the CAD mass spectrum of the ESI-generated $[M + H]^+$ (*m/z* 209) of chalcone. The fragments form via elimination of H_2O, CO, and C_6H_6 (presumably benzene) as reported earlier [19] along with minor fragments of *m/z* 103, *m/z* 105, presumably benzoyl cation, and *m/z* 194, from loss of the CH_3 radical. A comparison of the CAD mass spectra of protonated chalcone and 3-phenylindanone (Table 1) reveals that both compounds give the same fragment ions (of *m/z* 194, 191, 181, 131, and 103). For the 3-phenylindanone case, however, the abundances of ions at *m/z* 191 and 181 are greatly reduced, indicating that these fragments originate from another ionic species. In addition, the absence of the *m/z* 105 ion suggests that the benzoyl cation seen in the CAD mass spectrum of protonated chalcone represents that fraction of $[M + H]^+$ ions that does not cyclize. Nevertheless, the overall commonality of fragmentation suggests that some fraction of protonated chalcone isomerizes via Nazarov cyclization to afford protonated 3-phenylindanone.

CA of the collision-generated *m/z* 181 ions $[M + H - CO]^+$ via MS^3 experiments (Table 2) affords three important fragment ions of *m/z* 166, 153, and 103, which arise by elimination of CH_3, C_2H_4, and C_6H_6, respectively. The CAD mass spectra of the *m/z* 181 fragment ions from protonated chalcone and 3-phenylindanone are similar, consistent with the proposed cyclization. In addition, CA of the *m/z* 181 ion obtained as $[M + H -$

Table 2. CAD mass spectra of the fragment ions of *m/z* 181

Precursor of *m/z* 181	Fragment ions: relative abundance			
	m/z 179	*m/z* 166	*m/z* 153	*m/z* 103
Chalcone	25	100	10	20
3-Phenyl-1-indanone	54	100	18	30
1,1-Diphenylethanol	8	100	14	16

Table 3. Partial metastable-ion (MI) mass spectra of CI produced $[M + H]^+$ ions

	Fragment ions: relative abundance				
Compound number	$-H_2O$	$-C_6H_6$	−Anisole (−Phenol†)	−Ketene (−Methyl Ketene*)	Benzoyl *m/z* 105
2	2	12	10	100	63
3	100	ND	10	*26	ND
4	8	8	10	16	100
5	4	50	22	ND	100
6	58	58	†30	ND	100

$H_2O]^+$ from protonated 1,1-diphenyl ethanol (**10**), selected as a suitable reference, exhibits the same fragments. The similarities indicate that the $[M + H - CO]^+$ fragment ions from both protonated chalcone and 3-phenylindanone possess the 1,1-diphenylethylcation structure, Table 2.

*2-Methoxychalcone (**2**)*

The ESI-generated $[M + H]^+$ ion of 2-methoxy chalcone (*m/z* 239) (**2**) fragments upon collisional activation to yield a dominant *m/z* 197 ion formed by elimination of 42 u (Table 1). The accurate mass of the fragment ion, 197.0965, corresponds to $C_{14}H_{13}O$ (calculated mass = 197.0966), indicating that the expelled neutral is C_2H_2O, likely ketene. The dominant loss of ketene contrasts significantly with the fragmentations observed for protonated chalcone.

The metastable-ion (MI) decompositions of the CI-generated $[M + H]^+$ of **2** (*m/z* 239) (Table 3) yield *m/z* 207, 197, 161, and 131 fragments formed by losses of methanol, ketene, and the elements of benzene and anisole, respectively. (Similar results were obtained for high-energy CAD of CI-generated $[M + H]^+$ of **2**.) We note that CI produces ions with greater internal energy than ESI, explaining the lack of *m/z* 207, 161, and 131 fragments in the ESI low-energy CAD mass spectrum (Table 1) and indicating that these latter ions are formed by higher energy processes than that giving the *m/z* 197 ion, which is likely produced by a low-energy rearrangement. High-energy CAD of the *m/z* 197 fragment ion affords fragments ions at *m/z* 181, 165, 152, and 91 (Figure 1a). Given that the *m/z* 91 ion (benzyl or tropylium) corresponds to the base peak, the *m/z* 197 fragment must have a structure from which the $C_7H_7^+$ cation can be readily generated.

Furthermore, high-energy CAD of the $[M + D]^+$ ion (*m/z* 240) of Compound **2** generated by CD_4 CI shows that $[M + D]^+$ dissociates by eliminating ketene rather than ketene-d_1, (*m/z* 198) indicating that the deuterium remains solely part of the product ion in the elimination of ketene. High-energy CA of the *m/z* 197 ion (Figure 1b) yields major fragments of *m/z* 181 (due to loss of CH_4), 165 (loss of CH_3OH), and 91 (formation of $C_7H_7^+$), which are all shifted upward by one *m/z* upon CA of the *m/z* 198 ion (Figure 1c). These results suggest that the initial D of *m/z* 240 has become one of the aromatic protons of the *m/z* 198 ion, specifically on the unsubstituted phenyl ring. We postulate that the likely structure of the *m/z* 197 ion is that of the 2-methoxyphenyl-phenyl-methyl cation and the $C_7H_7^+$ is consequently the benzyl cation.

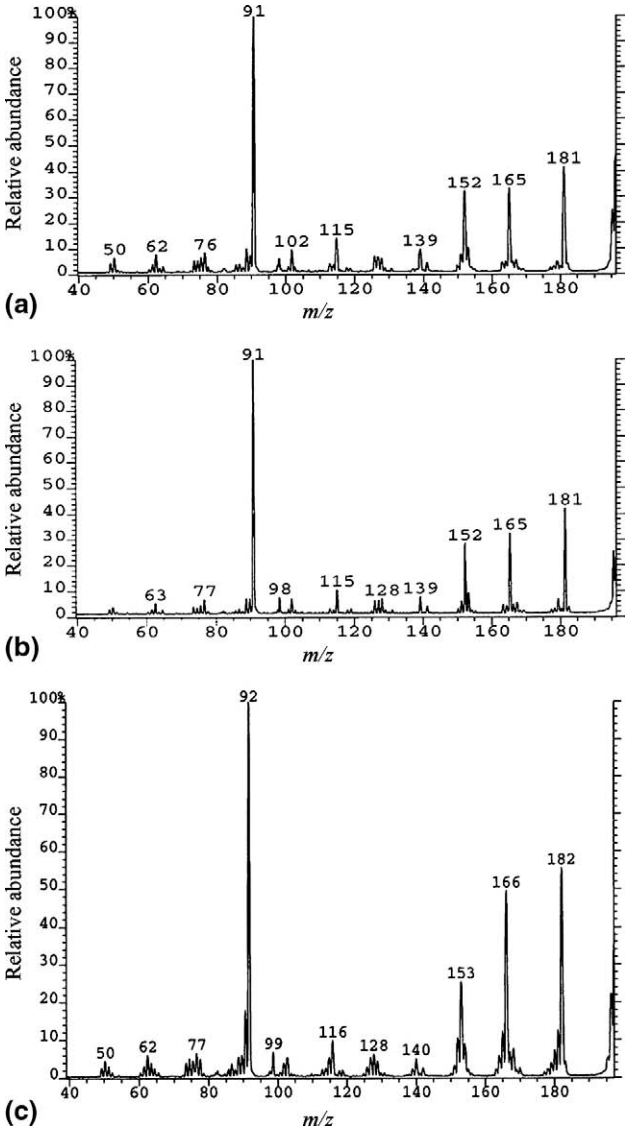

Figure 1. CAD mass spectra of (**a**) ion *m/z* 197 from **2** (**b**) *m/z* 197 ion from **3,** (**c**) ion *m/z* 198 from $[M + D]^+$ of **2**. Instrument: BEBE tandem sector.

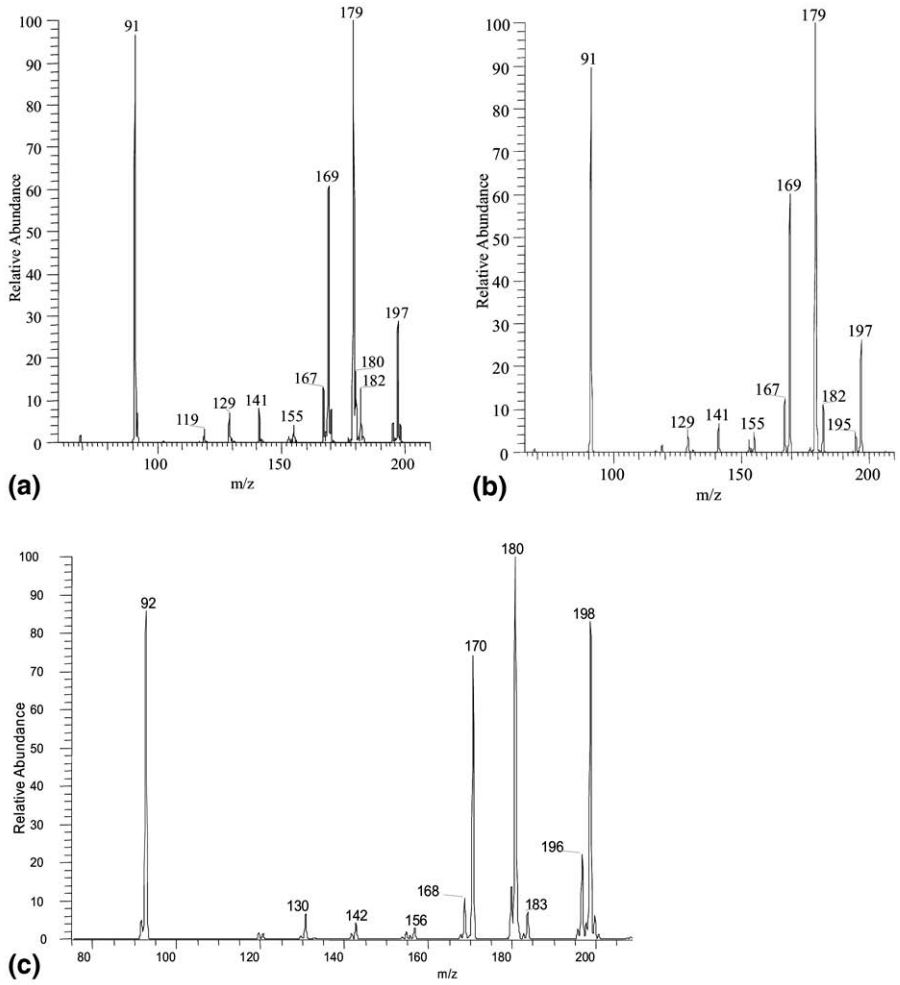

Figure 2. CAD mass spectra of (**a**) *m/z* 197 from 2-methoxy chalcone (**2**), (**b**) *m/z* 197 from 2-methoxybenzhydrol (**8**), (**c**) *m/z* 198 from $[M + D]^+$ of **2**. (All are MS^3 experiments). Instrument: 3D ion trap.

We generated a suitable reference for the *m/z* 197 ion having the 2-methoxyphenyl-phenyl-methyl cation structure by low-energy CA of the ESI-generated $[M + Na]^+$ ion of 2-methoxybenzhydrol (**8**). Others have reported generating 2-methoxyphenyl-phenyl-methyl cation by loss of H_2O from the CI-generated $[M + H]^+$ ion of **8** and producing its CAD mass spectrum via an ion trap instrument, which shows an abundant fragment of *m/z* 91 (benzyl cation) [42]. Furthermore, they reported an $C_7H_5D_2^+$ ion as a CAD fragment of the OCD_3 analog (*m/z* 200), derived by the loss of H_2O from protonated 2-d_3-methoxybenzhydrol, thus indicating that the methylene moiety of the benzyl cation is derived from the OCH_3 group.

Low-energy CA (Figure 2a) of the collision-generated *m/z* 197 fragment via an MS^3 experiment involving 2-methoxychalcone (**2**) compares well with that of the *m/z* 197 ion (MS^3 experiment) from Compound **8** (Figure 2b). The strong similarity indicates that the $[M + H - CH_2CO]^+$ ion from Compound **2** is the 2-methoxyphenyl-phenyl-methyl cation (eq 1). Low-energy CA in an MS^3 experiment involving the *m/z* 197 ion (Figure 2a) causes losses of H_2O and CO (forming *m/z* 179 and 169 ions, respectively) and formation of the *m/z* 91 ion. The *m/z* of these fragments increases by one for the *m/z* 198 intermediate $[M + D - CH_2CO]^+$ (Figure 2c). Similar product-ion *m/z* shifts occur upon high-energy CA of the CI-produced *m/z* 198 ion (Figure 1c). The facile losses of H_2O and CO likely indicate substantial but low-energy rearrangement processes, whereas the losses of CH_4 and CH_3OH (Figure 1a) induced by high-energy MS/MS experiments are more direct, higher energy processes. In either case, the production of the *m/z* 91 ion is a dominant process exhibiting identical deuterium-labeling results.

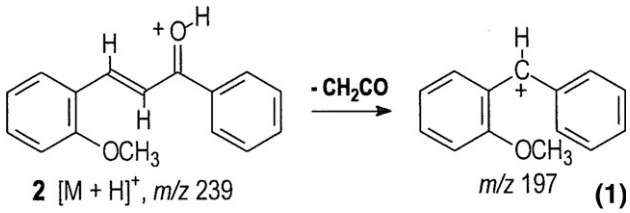

2 $[M + H]^+$, *m/z* 239 *m/z* 197 **(1)**

2-Methoxy-β-Methyl-Chalcone (3)

We chose to examine the CAD mass spectrum of the ESI-produced $[M + H]^+$ ion of β-methyl analogue, 2-methoxy-β-methyl-chalcone (**3**) to determine the origin of the ketene. The $[M + H]^+$ expectedly dissociates via elimination of methyl ketene to afford the *m/z* 197 ion (Table 1). Its accurate mass is 197.0964, in good agreement with the calculated mass of $[M + H - CH_3CH{=}C{=}O]^+$. The other major fragment ion is $[M + H - H_2O]^+$ (measured mass, 235.1129; calculated for $C_{17}H_{15}O$, 235.1123), which is likely facilitated by the protons on the β-methyl group.

The MI and high-energy CAD mass spectra of the CI-generated $[M + H]^+$ of **3** (Table 3) exhibit peaks corresponding to *m/z* 235, 197, and 145 ions, formed by expulsions of H_2O, methyl ketene (56 u) and $CH_3OC_6H_5$ (108 u), respectively. Moreover, CA of the *m/z* 197 ion obtained by CI protonation of Compounds **2** and **3** (Figure 1a, b) gives similar results, indicating that the *m/z* 197 fragments from both compounds have the same structure, namely, the 2-methoxyphenyl(phenyl)methyl cation formed by similar reaction (eq 2). These observations indicate that the $[M + H]^+$ of Compound **3** eliminates methylketene by a mechanism analogous to that for loss of ketene from protonated **2** and that the β carbon along with the adjacent carbonyl group form the ketene core.

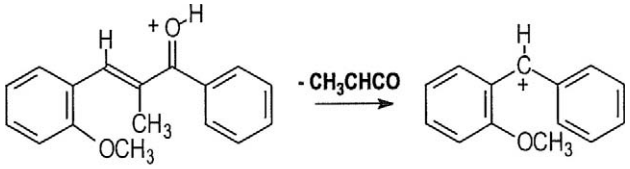

3 $[M + H]^+$, *m/z* 253 *m/z* 197 **(2)**

2-Hydroxy-Chalcone (4)

To delineate the role of methoxy in the elimination of ketene, we replaced the *ortho* OCH_3 by OH and protonated the 2-hydroxy-chalcone by CI and ESI. The MI dissociations of the CI-generated $[M + H]^+$ (*m/z* 225) are losses of H_2O, ketene, and C_6H_6 (giving *m/z* 207, 183, and 147 ions, respectively) (Table 3). CA of the ESI-generated $[M + H]^+$ (Table 1) causes ketene elimination and formation of the benzoyl cation at *m/z* 105; the presence of the highly abundant *m/z* 183 ion and the absence of the *m/z* 207 and 147 ions suggest that loss of ketene is a lower energy process than losses of H_2O and C_6H_6, as is also the case for 2-methoxy-chalcone (**2**).

By analogy to the structure of the $[M + H - CH_2CO]^+$ fragment from 2-methoxy chalcone, we propose that the *m/z* 183 fragment is the 2-hydroxyphenyl-phenyl-methyl cation (eq 3). As a reference, we synthesized 2-hydroxybenzhydrol (**9**) that, upon protonation by ESI followed by CA, loses water to give the desired *m/z* 183 fragment. Low-energy CA of the ion from **6** (Figure 3a) and from its reference **9** (Figure 3b, Table 4) MS^3 gives similar spectra, indicating that the two *m/z* 183 ions have the 2-hydroxyphenyl-phenyl-methyl cation structure [43]. Hence, the elimination of ketene from **4** follows a mechanism analogous to that for its elimination from **2**, indicating that the OH group plays a nearly identical role as OCH_3 in elimination of ketene.

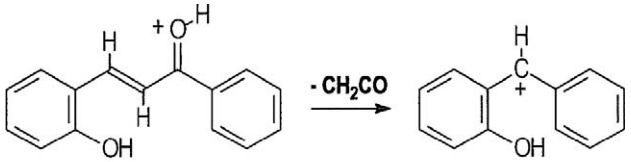

4 $[M + H]^+$, *m/z* 225 *m/z* 183 **(3)**

The $[M + H]^+$ of **4** has two OH groups (assuming protonation on the carbonyl oxygen), and hence H/D exchange/scrambling is possible in the corresponding $[M + D]^+$ ion so that the D may be present as phenolic OD for some fraction of the $[M + D]^+$. Given that H^+-shifts can be mediated by the oxygen atom of the phenolic group, both retention and loss of deuterium accompanying formation of the product ions are expected. High-energy CA of CI-generated $[M + D]^+$ of *m/z* 226 from **4** does indeed produce *m/z* 183 and 184 ions in the abundance ratio of ~1:2, confirming that H/D exchange occurs and that both ketene and ketene-d_1 are eliminated. CA of ESI-generated $[M - H + 2D]^+$ ion of *m/z* 227 from **4** (Figure 4) gives *m/z* 183, 184, and 185 ions owing to eliminations of ketene-d_2, ketene-*d*, and ketene in ratio of ~1:3:1, indicating H/D scrambling before ketene elimination. The formation of ketene-d_2 along with the ratios of deuteria in the ketene elimination products indicate that, in addition to the two hydroxyl hydrogens, two other hydrogen are involved in scrambling. The proton of the *ortho* OH group must somehow initiate H/D scrambling, something that the otherwise similar *ortho* OCH_3 (from **2**) cannot.

In summary, protonated 2-methoxy (**2**) or 2-hydroxychalcone (**4**) precursors decompose predominantly upon CA by ketene elimination to give 2-methoxy or 2-hydroxyphenyl-phenyl-methyl cations, respectively. This process requires a 1,3-migration or equivalent of the unsubstituted phenyl from the carbonyl carbon to the α carbon. Furthermore, the loss of methylketene from protonated 2-methoxy-β-chalcone (**3**) implies that the β-olefinic carbon, adjacent to the carbonyl group, is eliminated as part of the ketene in these systems. Finally, fragmentation of the $[M + D]^+$ of (**2**) via ketene loss proceeds with complete retention of the D on the product *m/z* 198 ion, which fragments to yield benzyl ion (*m/z* 92) also with D retention, implying that the initial D is transferred from the presumptive site of charging, the carbonyl oxygen, to an aryl site on the unsubstituted phenyl **'b'** ring. To accommodate these three mechanistic criteria, we propose that the protonated 2-methoxy and 2-hydroxy-chalcones undergo, upon activation, Nazarov cyclizations to give protonated 3-aryl-indanones from which ketene is eliminated

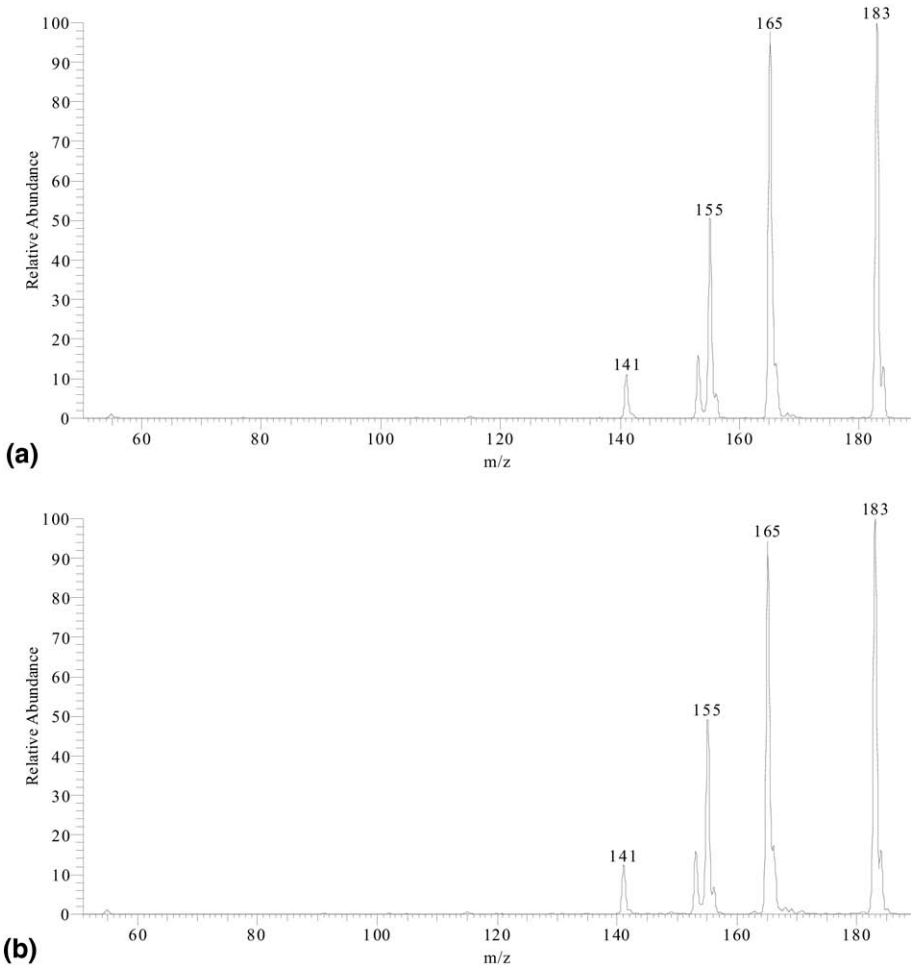

Figure 3. **(a)** The CAD MS of fragment ion of m/z 183 obtained by MS^3 experiment on the ESI produced $[M + H]^+$ of Compound **5**. **(b)** The CAD MS of fragment ion of *m/z* 183 obtained by MS^3 experiment on the ESI produced $[M + H]^+$ of Compound **11.**

(eq 4). In addition, the 2-methoxy/2-hydroxy groups must play a crucial role for both the Nazarov cyclization and ketene loss because the unsubstituted chalcone, when protonated, gives only partial cyclization with no observable ketene loss.

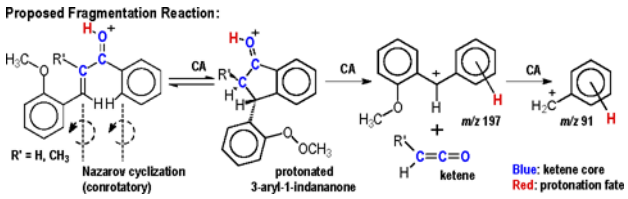

2-Chlorochalcone (**7**)

We designed a test for the hypothesis by investigating a chalcone with a less basic *ortho* substituent to delineate better the requirements for the cyclization and loss of ketene. CA of the $[M + H]^+$ of 2-chlorochalcone shows that it fragments to yield *m/z* 225, 215, 165, and 131 ions by eliminations of H_2O, CO, C_6H_6, and C_6H_5Cl, respectively, analogous to the fragmentations of chalcone (Table 1). The *m/z* 201 fragment produced by ketene elimination, however, is only 2%, indicating that the poorly basic Cl group is less capable than OCH_3 and OH in catalyzing cyclization and ketene elimination.

Table 4. CAD mass spectra of collisionally generated ions of *m/z* 183

	Relative abundances of the fragment ions			
Precursor	*m/z* 165	*m/z* 155	*m/z* 153	*m/z* 141
2-Hydroxychalcone (**4**)	100	52	16	12
2-Hydroxybenzhydrol (**9**)	100	51	16	13

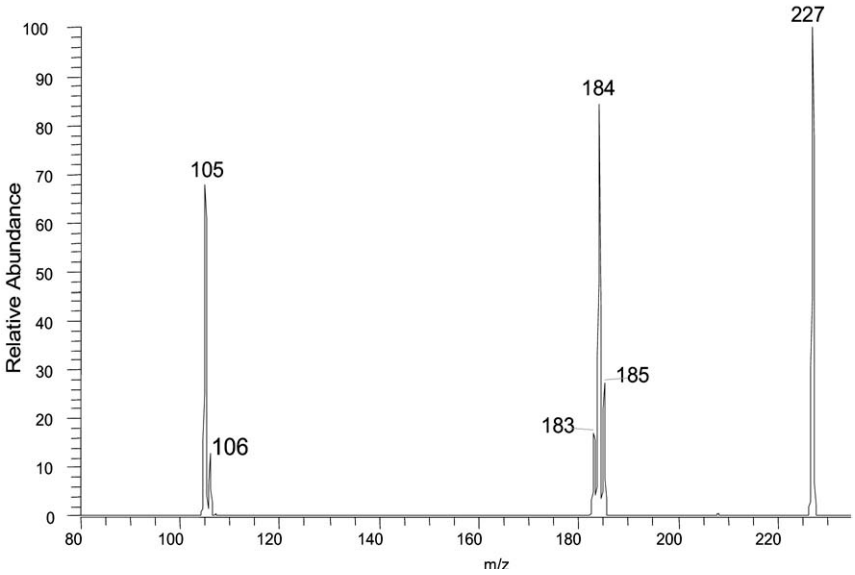

Figure 4. CAD mass spectrum of [2-hydroxychalcone − OH + 2D]+. Instrument: 3D ion trap.

Hence, there seems to be a minimum basicity requirement for the promotion of cyclization and the elimination of ketene. In addition, the low abundances of benzoyl cation (4%) and of fragments arising from elimination of H_2O or CO suggest that some fraction of the protonated **7** cyclizes by analogy to protonated chalcone.

*4-Methoxychalcone (**5**) and 4-Hydroxychalcone (**6**)*

To explore other criteria for cyclization, we examined 4-methoxychalcone (**5**) and 4-hydroxychalcone (**6**) using CI and ESI to protonate the neutral molecules. The MI dissociations of the CI-generated $[M + H]^+$ from **5** and **6** give rise to not only the benzoyl cation but also other fragments formed by eliminations of H_2O, C_6H_6, and substituted C_6H_6 analogous to eliminations from protonated unsubstituted chalcone; no detectable elimination of ketene occurs. CA of the ESI-produced $[M + H]^+$ ions also produces benzoyl cations and other fragment ions formed by the eliminations of H_2O, CO, and C_6H_6, and substituted C_6H_6 as established by accurate mass measurements (Table 5), but again no detectable elimination of ketene. By analogy to unsubstituted chalcone, a small fraction of protonated **5** and **6** may also cyclize to substituted indanones; the lower abundance of the benzoyl cation generated when ESI was used for protonation compared with when CI was used, and MI spectra taken (Table 1 and 3) indicates that cyclization takes place to a greater extent upon protonation by ESI. Overall, the results for protonated **5** and **6** relative to **2** and **4** clearly demonstrate the necessity of the *ortho* substitution for the promotion of Nazarov cyclization and subsequent elimination of ketene.

Proposed Mechanisms and Theoretical Calculations

Theory: Protonated Chalcone

We undertook theoretical calculations to aid in the elucidation of fragmentation mechanisms and the role of cyclization. Specific subjects are protonation, feasibility of cyclization, and subsequent fragmentation of protonated chalcone (**1**), 2-methoxy-chalcone (**2**), and 2-hydroxy-chalcone (**9**). Calculations reveal that the lowest-energy protonation of $[M + H]^+$ ions occurs on carbonyl oxygen in all three cases. We chose these initial forms, $\mathbf{A_1}$, as the reference points for calculat-

Table 5. Accurate masses of the fragment ions of Compounds **5** and **6**

Compound	Nominal mass	Measured mass	Molecular formula	Calculated mass	Neutral lost
4-Methoxy chalcone (**5**)	221	221.0969	$C_{16}H_{13}O$	221.0966	H_2O
	211	211.1141	$C_{15}H_{15}O$	211.1123	CO
	161	161.0601	$C_{10}H_9O_2$	161.0602	C_6H_6
4-Hydroxy chalcone (**6**)	207	207.0801	$C_{15}H_{11}O$	207.0809	H_2O
	197	197.0971	$C_{14}H_{13}O$	197.0966	CO
	147	147.0440	$C_9H_7O_2$	147.0445	C_6H_6

Table 6. Calculated relative enthalpies of formation/reaction (Scheme 1, in kJ/mol)

Minima	Chalcone	2-Hydroxy chalcone	2-Methoxy chalcone	Transition states	Chalcone	2-Hydroxy chalcone	2-Methoxy chalcone
Label	Δ^2H_f	Δ^2H_f	Δ^2H_f	Label	$\Delta^2H^{\ddagger}$	$\Delta^2H^{\ddagger}$	$\Delta^2H^{\ddagger}$
A_1	0	0	0	TS (A_1-A_2)	140	129	120
A_2	21	23	22	TS (A_2-A_3)	55	64	67
A_3	39	41	41	TS (A_3-B_1)	154	154	156
A_4	3	4	4	TS (B_1-B_2)	257	258	260
A_5		3	4	TS (B_2-C_3)	214	198	199
B_1	123	131	134	TS (C_3-C_6)	47	35	42
B_2	194	195	191	TS (A_1-A_4)	124	54	58
C_1	116	121	125	TS (A_4-C_1)	204	127	129
C_2	116	133	130	TS (C_1-C_2)	157	220	220
C_3	−10	−3	1	TS (C_2-C_3)		174	174
C_4		115	118	TS (A_4-A_5)		56	60
C_5		139	120	TS (A_5-C_4)		127	129
C_6	$=C_3$	−9	−3	TS (C_1-C_4)		144	152
				TS (C_4-C_5)		138	128
				TS (C_5-C_6)		146	123
				TS (C_5-C_6)u		147	

‡The enthalpies of formation of the various transition structures.

ing relative enthalpies of formation and reaction in Tables 6, and 7.

In addition to $\mathbf{A_1}$, there is an ensemble of other uncyclized forms related by rotations about various bonds between the two phenyl rings and by proton transfers ($\mathbf{A_i}$ of the Schemes). The formation of protonated 3-aryl-1-indanones from these precursors via Nazarov cyclization in the gas phase would require the equivalent of a 1,3-H^+ transfer after the conrotatory cyclization. We could not find this transition state and, even if it did exist, it probably would require substantial energy to cross such that other processes would predominate. As shown on Scheme 1, there are three other routes (Figure 5) to accomplish that equivalent of this H-transfer. Route **1**, $\mathbf{A_1} \rightarrow \mathbf{A_2} \rightarrow \mathbf{A_3} \rightarrow \mathbf{B_1} \rightarrow \mathbf{B_2} \rightarrow \mathbf{C_3} \rightarrow \mathbf{C_6}$, involves a pair of 1,2-H^+ transfers, however, the transition-state **TS($\mathbf{B_1}$-$\mathbf{B_2}$)** still requires >250 kJ/mol additional energy to surmount (Table 6). On Route **2**, $\mathbf{A_1} \rightarrow \mathbf{A_4} \rightarrow \mathbf{C_1} \rightarrow \mathbf{C_2} \rightarrow \mathbf{C_3} \rightarrow \mathbf{C_6}$, which requires a pair of 1,4-H^+ transfers, the greatest barrier is transition-state **TS($\mathbf{C_1}$-$\mathbf{C_2}$)**, which requires 200 to 220 kJ/mol additional energy. Route **3**, $\mathbf{A_1} \rightarrow \mathbf{A_4} \rightarrow \mathbf{A_5} \rightarrow \mathbf{C_4} \rightarrow \mathbf{C_5} \rightarrow \mathbf{C_6}$, requires a pair of favorable 1,5-H^+ transfers involving the *ortho* substituent and, in contrast, presents maximum barriers on trajectory from $\mathbf{A_5}$ to $\mathbf{C_6}$ that require <160 kJ/mol additional energy. In addition, calculations reveal that the protonated 3-aryl-1-indanones are the most stable structures on the potential energy surface from protonated chalcones to the elimination of ketene.

Route **3**, the most favorable route through cyclization to the protonated 3-aryl-1-indanones (Figure 5 illustrating 2-methyoxychalcone case), constitutes an example of intramolecular proton-catalyzed transport [21–24] where the transport mediator is the oxygen of the 2-hydroxy or 2-methoxy groups. Since Route **3** in not available for the unsubstituted chalcone case, conversion to protonated 3-aryl-1-indanone then would be by

Table 7. Calculated relative enthalpies of formation and reaction (Scheme 2, in kJ/mol)

Minima	Chalcone	2-Hydroxy chalcone	2-Methoxy chalcone	Transition states	Chalcone	2-Hydroxy chalcone	2-Methoxy chalcone
Label	Δ^2H_f	Δ^2H_f	Δ^2H_f	Label	$\Delta^2H^{\ddagger}$	$\Delta^2H^{\ddagger}$	$\Delta^2H^{\ddagger}$
C_7		119	98	TS (C_6-C_7)		122	103
C_8	−6	−5	1	TS (C_7-G_1)		133	126
C_9	118	119	124	TS (C_6-C_8)	41	42	47
G_1	124	117	121	TS (C_8-C_9)	214	213	217
G_2	113	115	119	TS (C_9-G_1)	173	169	175
G_3		111	97	TS (G_1-G_2)	127	126	132
IDC_K	102	112	115	TS (G_2-G_3)		121	126
				TS (G_3-H_1)		141	142
				TS (G_2-H_1)	137	142	144
Label	Δ^2H_{rx}	Δ^2H_{rx}	Δ^2H_{rx}				
H_1 + K	117	126	124				

‡The enthalpies of formation of the various transition structures.

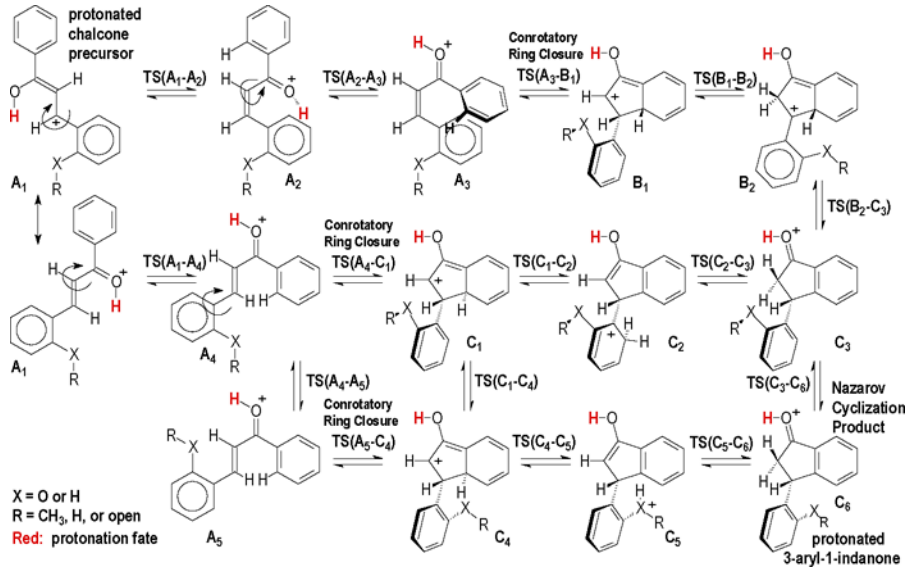

Scheme 1. Proposed mechanism, formation of protonated 3-aryl-indanone from protonated chalcone precursor.

Route **2** requiring 204 kJ/mol, hence cyclization for the unsubstituted chalcone would be less competitive and only partially complete, as observed experimentally. The most favorable Route **3** would also not be available for the 4-hydoxy and 4-methoxy isomers for geometric reasons, explaining why these isomers exhibit similar fragmentation features as the unsubstituted chalcone. A critical requirement for intramolecular proton-catalyzed transport of Route **3** is the presence of an *ortho* substituent of sufficient basicity to abstract a proton from the C9 (former C2′) position for subsequent transfer to the C2 (former β) position. The calculated relative enthalpies of formation for $\mathbf{C_4}$, $\mathbf{C_5}$, and connecting transition-state **TS($\mathbf{C_4}$–$\mathbf{C_5}$)** show additional investment <25 kJ/mol to accomplish a feasible proton transfer to the 2-hydroxy and 2-methoxy moieties (Table 6). In contrast, $\mathbf{C_5}$ for the 2-chloro substituent is not stable, and thus would be less efficient as an agent for proton-catalyzed transport [22].

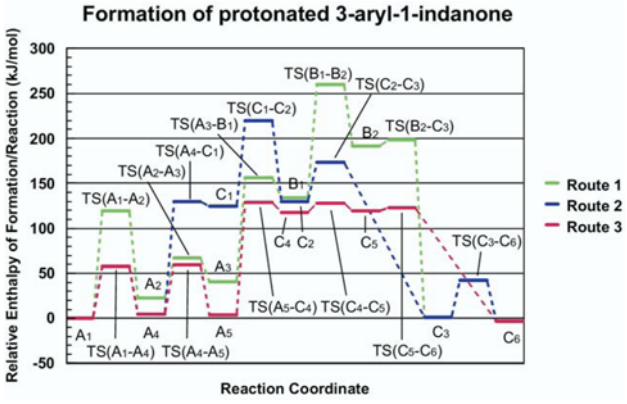

Figure 5. Comparative enthalpies of formation along reaction routes to protonated 3-aryl indanone formation (2-methyoxychalcone case).

The elimination of ketene from the protonated 3-aryl-1-indanones [e.g., from (**2**) and (**4**)], requires the translocation of the proton on the carbonyl oxygen to somewhere on the phenyl ring (former **'b'** ring), as required by the D labeling results, particularly in the 2-methoxy case (**2**) where no d_1-ketene loss occurs. Two routes are available (Scheme 2, Figure 6). Route **A** involves transfer of proton from the carbonyl oxygen to C7 and then to C8, $\mathbf{C_6} \rightarrow \mathbf{C_8} \rightarrow \mathbf{C_9} \rightarrow \mathbf{G_1}$ where **TS($\mathbf{C_8}$-$\mathbf{C_9}$)** requires >210 kJ/mol additional energy to surmount. In contrast, route **B**, $\mathbf{C_6} \rightarrow \mathbf{C_7} \rightarrow \mathbf{G_1}$ presents a maximum barrier of'~130 kJ/mol to same intermediate ($\mathbf{G_1}$). On route **B**, the OCH_3, and OH groups act as intramolecular proton transfer catalysts; the ionizing H^+ on the carbonyl group is first abstracted to the 2-methoxy or 2-hydroxyl group and then transferred to the C8 position (former C1′ on the **'b'** ring), activating the adjacent C–C bond for cleavage to $\mathbf{G_2}$. The basicity of the *ortho* OCH_3 and OH groups is necessary for efficient proton transfer catalysis (Table 7), something that an *ortho* Cl cannot perform because corresponding intermediate $\mathbf{C_7}$ is unstable. From $\mathbf{G_2}$ are two energetically similar paths, one direct and another through a cyclic intermediate $\mathbf{G_3}$, resulting in formation an ion–dipole complex, $\mathbf{IDC_K}$, preparatory to elimination of ketene. The ionizing proton thus is translocated to the *ortho* position of the unsubstituted phenyl group in the product ion $\mathbf{H_1}$, in accord with D^+ labeling results The ketene loss via proton transport catalysis is so facile that it suppresses any other fragmentations routes for the protonated 3-(2-methoxy) phenyl-1-indanone intermediate, whereas

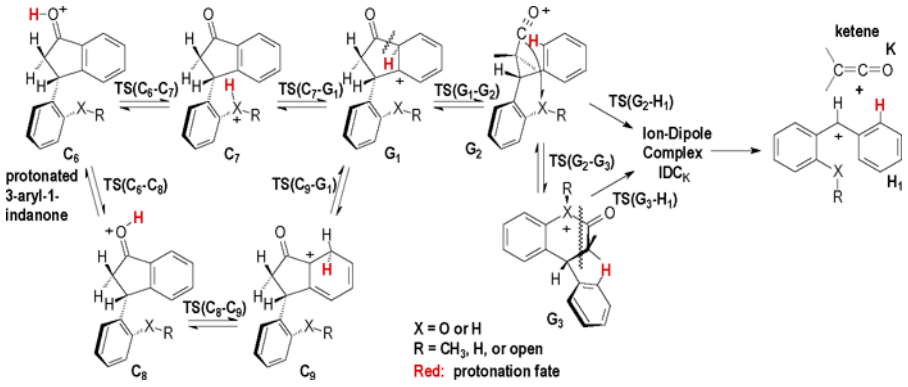

Scheme 2. Proposed mechanism, elimination of ketene from protonated 3-aryl-1-indanone.

ketene loss is not observed for protonated 3-phenyl-1-indanone.

The 2-hydroxy analog (**4**) differs from the 2-methoxy case in several important ways. First, there is a much greater abundance of the *m/z* 105 ion in the ESI CAD mass spectrum of **4** (Table 1) compared with that of 2-methoxychalcone under identical conditions (same instrument and collision energy). Second, H/D scrambling occurs in both high-energy CAD of the CI-produced $[M + D]^+$ and low-energy CAD of the ESI-produced $[M - H + 2D]^+$ whereas no H/D exchange is detectable for the 2-methoxy analogue (**2**). We rationalize these differences by a proposed mechanism (Scheme 3) whereby the protons of the 2-OH groups and the β-C-H site are interchanged becoming equivalent with regard to H/D labeling. This interchange is initiated by the phenol OH, which is not possible for the 2-methoxy analogue. A fourth proton, at C2′ of the **'b'** ring (C9 after cyclization), becomes involved in that both protons on the $R-OH_2^+$ moiety of intermediate C5 (Scheme 1) can be transferred to the C6 site (former β-C) by virtually equal barriers, **TS(C_5-C_6)** versus **TS(C_5-C_6)u** (Table 6). This process is also unavailable to the 2-methoxy analogue. The resulting H/D distribution would be 1:2 for d_1/d_0-ketene elimination from $[M + D]^+$, as is observed, and 1:4:1 for $d_2/d_1/d_0$-ketene from $[M - H + 2D]^+$, which is close to the experimental ~1:3:1. Thus, the labeling results provide strong confirmation for the proposed mechanisms. In addition, generation of *m/z* 105, the benzoyl cation, is accomplished by direct cleavage of $\mathbf{A_8}$ with no reverse activation barrier.

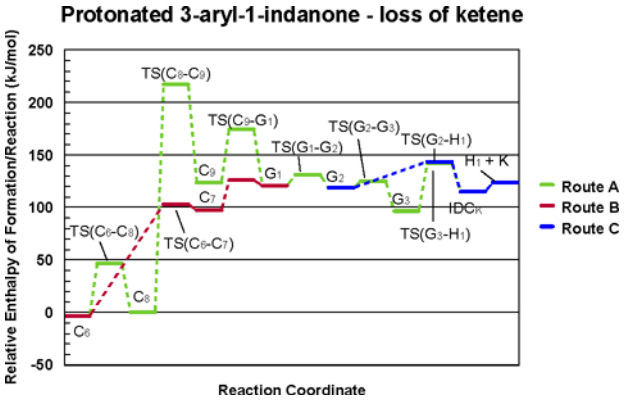

Figure 6. Comparative enthalpies of formation/reaction of ketene elimination from protonated 3-aryl indanone (2-methoxychalcone case).

Another type of cyclization is possible where the protonated carbonyl initiates an electrophilic attack upon the **'a'** ring (Scheme 4). The cyclic products thus generated are configured for ready elimination of H_2O. This route of elimination, however, requires greater energy than that for ketene elimination and appears to be competitive only for those compounds that do not have an *ortho* substituent to catalyze critical proton-catalyzed transports.

From the $[M + D]^+$ of 2-methyoxy-chalcone (**2**), the quantitative formation of the *m/z* 92 versus *m/z* 91 (Figure 2c) product ion from the collision-generated *m/z* 198 ion $[M + D - CH_2CO]^+$ clearly substantiates that D is present in the phenyl ring of *m/z* 198. This reaction belongs to the class of empirically-observed fragmentations from substituted diphenylcarbinols and diphenylmethyl cations [42, 43]. We have verified the basic postulated mechanism by theoretical calculations; the *m/z* 197 ion decomposes to give the *m/z* 91 ion benzyl cation formed by the mechanism in Scheme 5. An addition to the original proposed mechanism revealed by theoretical calculations is the formation of an ion-dipole complex, $\mathbf{IDC_Q}$, in the fragmentation exit channel to products. The mechanism preserves the location of the charging proton at the *ortho* position of the unsubstituted phenyl ring where it is remote to exchange reactions.

Further information regarding the theoretical calculations is available in the Supplementary Materials.

Conclusions

Although a Nazarov-type cyclization likely occurs to some extent for protonated chalcone, this process becomes of high yield for the protonated 2-hydroxy and 2-methoxy chalcones (Scheme 1). The intermediate products are protonated 3-aryl-1-indanones. A key finding is that OCH_3 and OH groups at the *ortho* position act as proton-transfer catalysts, in that they

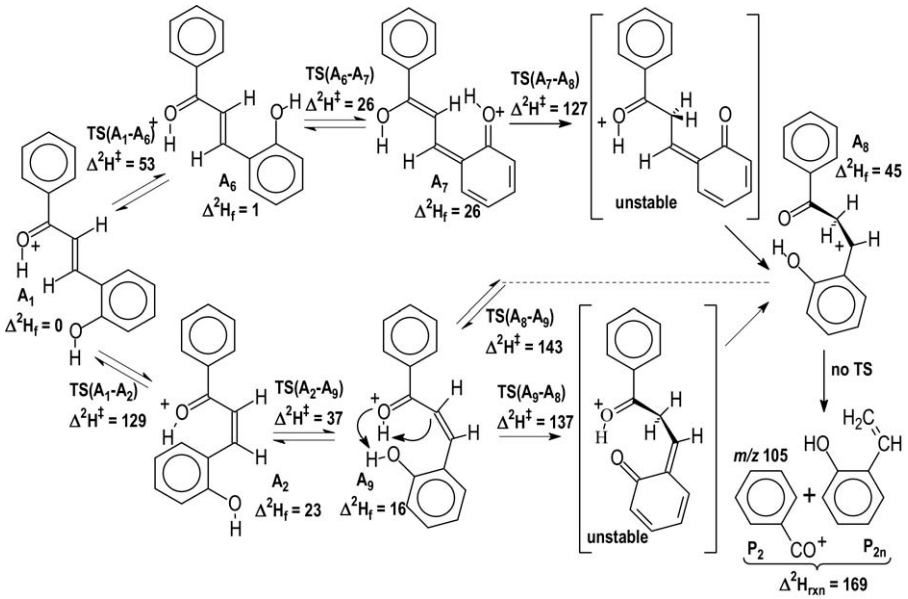

Scheme 3. Proposed mechanism involved in H/D scrambling in protonated 2-hydroxychalcone.

decrease the activation energy for the equivalent 1,3 proton shift, a key step. Subsequently, ketene elimination occurs by a second, key 1,3 proton-shift (Scheme 2) similarly catalyzed by the oxygen atom of the *ortho* OCH_3 or OH groups. When the OCH_3 or OH groups, however, are absent from the *ortho* position, Nazarov-type cyclization takes place to a significantly lesser extent, and must compete with another type of cyclization. In addition, competitive expulsions of CO, H_2O, and C_6H_6 (or substituted C_6H_6) take place instead of ketene, which are also characteristic of protonated 3-phenyl-1-indanone. The structures of the $[M + H - \text{ketene}]^+$ and $[M + H - CO]^+$, as determined by comparison of their CAD mass spectra with those of reference ions, are consistent with these hypotheses. The proposed mechanisms find strong support from theoretical calculations using density functional theory and from accurate-mass data, tandem mass spectrometric experiments, and deuterium-labeling.

The gas-phase Nazarov cyclization of protonated chalcones is analogous to that occurring in solution. Its extent in the gas phase depends on the method used to protonate the starting material and on the nature and position of substituents. Moreover, the study shows that the cyclization and fragmentation of 2-methoxy and 2-hydroxy-chalocone are examples of *intramolecular proton-transport catalysis*.

Acknowledgments

V.S.S. and M.G. thank the KSCSTE for financial assistance, and Principal, Sacred Heart College, Thevara for providing infrastructure. R.S. thanks Dr. J. S. Yadav, Director, IICT, Hyder-

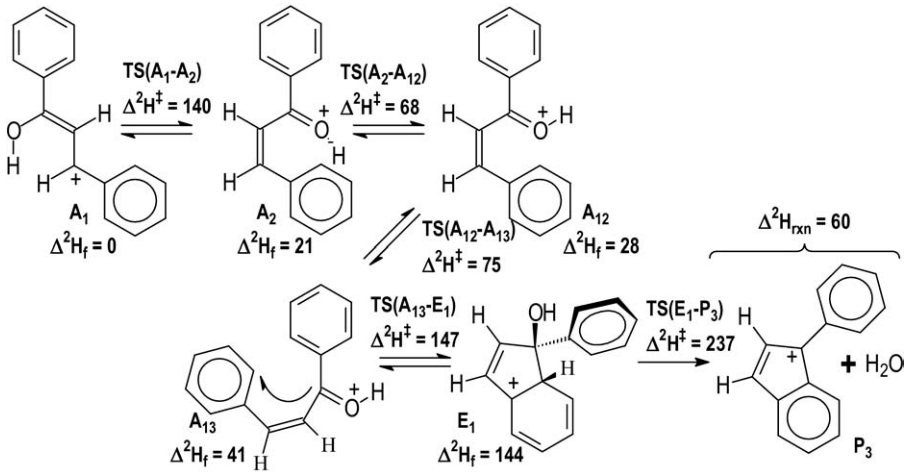

Scheme 4. Proposed alternate cyclization of protonated chalcone (**1**).

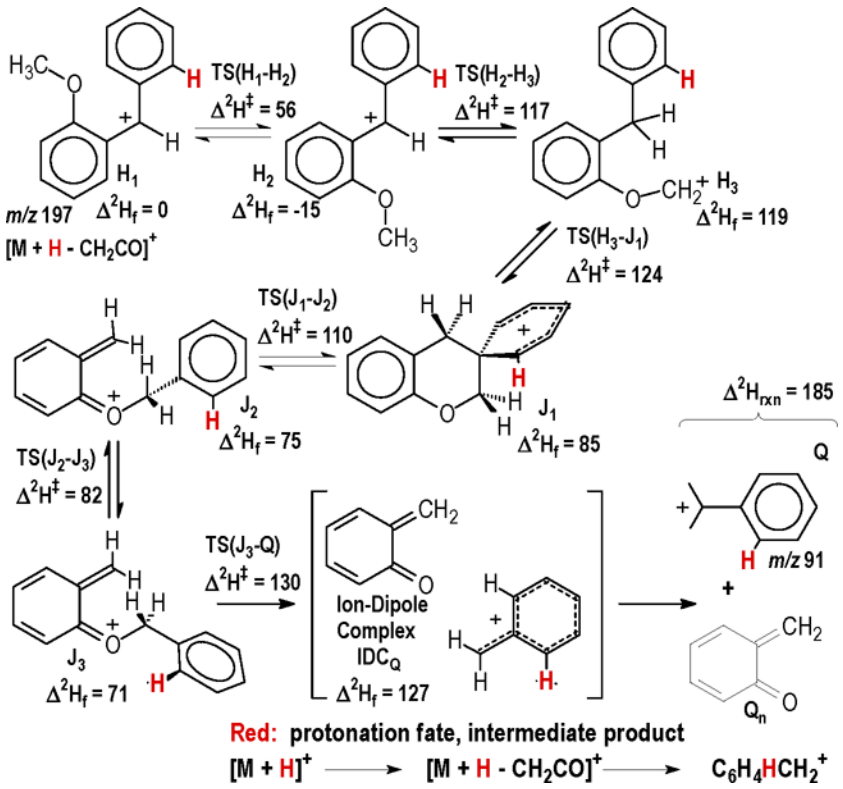

Scheme 5. Proposed mechanism, from *m/z* 197 to *m/z* 91 [42, 43]. Calculated enthalpies reported relative to $\mathbf{H_1}$ in kJ/mol.

abad, for facilities and Dr. M. Vairamani for cooperation. Research at WU was supported by the National Centers for Research Resources of the NIH, grant P41RR00954. In addition, this work made use of the Washington University Computational Chemistry Facility, supported by NSF grant CHE-0443501.

Appendix A
Supplementary Material

Supplementary material associated with this article may be found in the online version at doi:10.1016/j.jasms.2008.12.017.

References

1. Pellissier, H. Recent Developments in the Nazarov Process. *Tetrahedron* **2005,** *61,* 6479–6517.
2. Frontier, A.; Collinson, C. The Nazarov Cyclization in Organic Synthesis. Recent advances. *Tetrahedron* **2005,** *61,* 7577–7606.
3. Gu, X. H.; Yu, H.; Jacoboson, A. E.; Rothman, R. B.; Dersch, C. M.; George, C.; Flippen-Anderson, J. L.; Rice, K. C. Design, Synthesis, and Monoamine Transporter Binding Site Affinities of Methoxy Derivatives of Indatraline. *J. Med. Chem.* **2000,** *43,* 4868–4876.
4. Elliott, J. D.; Lago, M. A.; Cousins, R. D.; Leber, J. D.; Erhard, K. F.; Nambi, P.; Elshourbagy, M. A.; Kumar, C.; Lee, J. A.; Bean, J. W.; DeBrosse, C. W.; Eggleston, D. S.; Brooks, D. P.; Geuerstein, G.; Ruffolo, R. R. Jr.; Weinstock, J.; Gleason, J. G.; Peishoff, C. E.; Ohlstein, E. H. 1,3-Diarylindan-2-Carboxylic Acids, Potent and Selective Non-Peptide Endothelin Receptor Antagonists. *J. Med. Chem.* **1994,** *37,* 1553–1557.
5. Lawrence, N. J.; Simon, E.; Armitage, M.; Greedy, B.; Cook, D.; Ducki, S.; McGown, A. T. The Synthesis of Indanones Related to Combretastatin A-4 Via Microwave-Assisted Nazarov Cyclization of Chalcones. *Tetrahedron Lett.* **2006,** *47,* 1637–1640.
6. Yin, W.; Ma, Y.; Xu, J.; Zhao, Y. Microwave-Assisted One-Pot Synthesis of 1-Indanones from Arenes and α,β-Unsaturated Acyl Chlorides. *J. Org. Chem.* **2006,** *71,* 4312–4315.
7. Sivakumar, P. M.; Seenivasan, S. P.; Kumar, V.; Doble, M. Synthesis, Antimycobacterial Activity Evaluation, and QSAR Studies of Chalcone Derivatives. *Bioorg. Med. Chem. Lett.* **2007,** *17*(6), 1695–1700.
8. Beynon, J. H.; Lester, G. R.; Williams, A. E. Specific Molecular Rearrangements in the Mass Spectra of Organic Compounds. *J. Phy. Chem.* **1959,** *63,* 1861–1868.
9. Van De Sande, C.; Serum, J.; Vandwalle, W. Organic Mass Spectrometry. XII. Mass Spectra of Chalcones and Flavanones. Isomerization of 2′-Hydroxychalcone and Flavanone. *Org. Mass Spectrom.* **1972,** *6,* 1333–1346.
10. Ronayne, J.; Williams, D. H.; Bowie, J. H. Mass Spectrometry. XIX. Evidence for the Occurrence of Aromatic Substitution Reactions Upon Electron Impact. *J. Am. Chem. Soc.* **1966,** *88,* 4980–4984.
11. Rouvier, E.; Medina, H.; Cambon, A. Mass Spectrometric Studies. VIII. Fragmentation of Several Benzalacetophenones and Benzalacetones Variously Substituted on the Aromatic Ring. *Org. Mass Spectrom.* **1976,** *11,* 800–813.
12. Schaldach, B.; Grutzmacher, H. F. The Fragmentations of Substituted Cinnamic Acids After Electron Impact. *Org. Mass Spectrom.* **1980,** *15*(4), 175–181.
13. Kallury, R. K. M. R.; Loudon, A. G.; Maccoll, A. Electron Impact Studies on α,β-Unsaturated Carbonyl Oximes. *Org. Mass Spectrom.* **1978,** *13*(4), 218–223.
14. Ardanaz, C. E.; Kavka, J.; Curcuruto, O.; Traldi, P.; Guidugli, F. On the Structure of $[C_9H_6O]^+$ Ions Originating by Electron Impact Induced Decomposition of Chalcone. *Rapid Commun. Mass Spectrom.* **1991,** *5*(11), 569–573.
15. Ardanaz, C. E.; Traldi, P.; Vettori, U.; Kavka, J.; Guidugli, F. The Ion-Trap Mass Spectrometer in Ion Structure Studies. The Case of $[M - H]^+$ ions from chalcone. *Rapid Commun. Mass Spectrom.* **1991,** *5,* 5–10.
16. Tai, Y.; Pei, S.; Wan, J.; Cao, X.; Pan, Y. Fragmentation Study of Protonated Chalcones by Atmospheric Pressure Chemical Ionization and Tandem Mass Spectrometry. *Rapid Commun. Mass Spectrom.* **2006,** *20,* 994–1000.
17. Bohme D. K.; Schwarz, H. Gas-Phase Catalysis by Atomic and Cluster Metal Ions: The Ultimate Single-Site Catalysts. *Angew. Chem. Int. Ed.* **2005,** *44,* 2336–2354.
18. O'Hair, R. A. J. The 3D Quadrupole Ion Trap Mass Spectrometer as a Complete Chemical Laboratory for Fundamental Gas-Phase Studies of Metal Mediated Chemistry. *Chem. Commun.* **2006,** *14,* 1469–1481.
19. Kingston, E. E.; Beynon, J. H.; Liehr, J. G.; Meyrant, P.; Flammang, R.; Maquestiau, A. The Claisen Rearrangement of Protonated Allyl Phenyl Ether. *Org. Mass Spectrom.* **1985,** *20,* 351–359.

20. Moolayil, J. T.; George, M.; Srinivas, R.; Swamy, N. S.; Russell, A.; Giblin, D.; Gross, M. L. The Mass Spectrometry-Induced Cyclization of Protonated N-[2-(Benzoyloxy)Phenyl]-Benzamide: A Gas-Phase Analog of a Solution Reaction. *Int. J. Mass Spectrom.* **2006,** *249/250,* 21–30.
21. Bohme, D. K. Proton Transport in the Catalyzed Gas-Phase Isomerization of Protonated Molecules. *Int. J. Mass Spectrom. Ion Processes* **1992,** *115,* 95–110.
22. Chalk, A. J.; Radom, L. Proton-Transport Catalysis: A Systematic Study of the Rearrangement of the Isoformyl Cation to the Formyl Cation. *J. Am. Chem. Soc.* **1997,** *119,* 7573–7578.
23. Chalk, A. J.; Radom, L. Ion-Transport Catalysis: Catalyzed Isomerizations of NNH^+ and $NNCH_3^+$. *J. Am. Chem. Soc.* **1999,** *121,* 1574–1581.
24. Ruttink, P. J. A.; Burgers, P. C.; Fell, L. M.; Terlouw, J. K. Dissociation of Ionized 1,2-Ethanediol and 1,2-Propanediol: Proton-Transport Catalysis with Electron Transfer. *J. Phys. Chem.* **1998,** *102,* 2976–2980.
25. Trikoupis, M. A.; Terlouw, J. K.; Burgers, P. C. Enolization of Gaseous Acetone Radical Cations: Catalysis by a Single Base Molecule. *J. Am. Chem. Soc.* **1998,** *120*(46), 12131–12132.
26. Trikoupis, M. A.; Burgers, P. C.; Ruttink, P. J. A.; Terlouw, J. K. Benzonitrile Assisted Enolization of the Acetone and Acetamide Radical Cations: Proton-Transport Catalysis Versus an Intermolecular H+/D+ Transfer Mechanism. *Int. J. Mass Spectrom.* **2001,** *210/211,* 489–502.
27. Wang, X.; Holmes, J. L. A Study of the Isomerization and Dissociation of Formal $[Acetone\text{-}Methanol]^{+\cdot}$ Ion–Molecule Complexes. *Can. J. Chem.* **2005,** *83,* 1903–1912 and references therein.
28. Wang, X.; Holmes, J. L. Exploring the Potential Energy Surface of Ion-Molecule Pairs by Experiment and by Theory: Acetaldehyde and Methanol. *Int. J. Mass Spectrom.* **2005,** *242,* 75–85.
29. Sutton, R. Esters and Flavenes from 2-Hydroxychalcones and Flavylium Salts. *J. Org. Chem.* **1972,** *37*(7), 1069–1070.
30. Hendley, E. C.; Neville, O. K. Carbon14 Tracer Studies in the Rearrangements of Unsymmetrical α-Diketones. III. p-Methoxybenzylideneacetophenone Oxide. *J. Am. Chem. Soc.* **1953,** *75,* 1995–1996.
31. Becker, H. D.; Bremholt, T. Oxidative Rearrangement of *o*-Hydroxydiarylcarbinols. *Tetrahedron Lett.* **1973,** 6), 197–200.
32. Gross, M. L. Tandem Mass Spectrometry: Multisector Magnetic Instruments. In *Methods in Enzymology*, Vol. CXCIII, Mass Spectrometry. McCloskey, J. A., Ed. Academic Press: San Diego, 1990; p. 131–153.
33. Stewart, J. J. P.; Frank, J. S. Optimization of Parameters for Semi-Empirical Methods. I. Method. *J. Comp. Chem.* **1989,** *10,* 209–220.
34. Stewart, J. J. P.; Frank, J. S. Optimization of Parameters for Semi-Empirical Methods. II. Applications. *J. Comp. Chem.* **1989,** *10,* 221–264.
35. Wittbrodt, J. M.; Schlegel, H. B. Some Reasons Not to Use Spin Projected Density Functional Theory. *J. Chem. Phys.* **1996,** *105,* 6574–6577.
36. Baker, J.; Scheiner, A.; Andzelm, J. Spin Contamination in Density Functional Theory. *J. Chem. Phys. Lett.* **1993,** *216,* 380–388.
37. Laming, G. J.; Hardy, N. C.; Amos, R. D. Kohn-Sham Calculation on Open-Shell Diatomic Molecules. *Mol. Phys.* **1993,** *80,* 1121–1134.
38. Nicolaides, A.; Smith, D. M.; Jensen, F.; Radom, L. J. Phenyl Radical, Cation, and Anion. The Triplet-Singlet Gap and Higher Excited States of the Phenyl Cation. *J. Am. Chem. Soc.* **1997,** *119,* 8083–8088.
39. Frisch, M. J.; Trucks, G. W.; Schlegel, H. B.; Scuseria, G. E.; Robb, M. A.; Cheeseman, J. R.; Zakrzewski, V. G.; Montgomery, J. A. Jr.; Stratmann, R. E.; Burant, J. C.; Dapprich, S.; Millam, J. M.; Daniels, A. D.; Kudin, K. N.; Strain, M. C.; Farkas, O.; Tomasi, J.; Barone, V.; Cossi, M.; Cammi, R.; Mennucci, B.; Pomelli, C.; Adamo, C.; Clifford, S.; Ochterski, J.; Petersson, G. A.; Ayala, P. Y; Cui, Q.; Morokuma, K.; Malick, D. K.; Rabuck, A. D.; Raghavachari, K.; Foresman, J. B.; Cioslowski, J.; Ortiz, J. V.; Stefanov, B. B.; Liu, G.; Liashenko, A.; Piskorz, P.; Komaromi, I.; Gomperts, R.; Martin, R.L.; Fox, D. J.; Keith, T.; Al- Laham, M. A.; Peng, C. Y.; Nanayakkara, A.; Gonzalez, C.; Challacombe, M.; Gill, P. M. W.; Johnson, B.; Chen, W.; Wong, M. W.; Andres, J. L.; Gonzalez, C.; Head-Gordon, M.; Replogle, E. S.; Pople, J. A. *Gaussian* 98, Revision A6. Gaussian, Inc.: Pittsburgh PA, 1998.
40. Frisch, M. J.; Trucks, G. W.; Schlegel, H. B.; Scuseria, G. E.; Robb, M. A.; Cheeseman, J. R.; Montgomery, Jr., J. A.; Vreven, T.; Kudin, K. N.; Burant, J. C.; Millam, J. M.; Iyengar, S. S.; Tomasi, J.; Barone, V.; Mennucci, B.; Cossi, M.; Scalmani, G.; Rega, N.; Petersson, G. A.; Nakatsuji, H.; Hada, M.; Ehara, M.; Toyota, K.; Fukuda, R.; Hasegawa, J.; Ishida, M.; Nakajima, T.; Honda, Y.; Kitao, O.; Nakai, H.; Klene, M.; Li, X.; Knox, J. E.; Hratchian, H. P.; Cross, J. B.; Adamo, C.; Jaramillo, J.; Gomperts, R.; Stratmann, R. E.; Yazyev, O.; Austin, A. J.; Cammi, R.; Pomelli, C.; Ochterski, J. W.; Ayala, P. Y.; Morokuma, K.; Voth, G. A.; Salvador, P.; Dannenberg, J. J.; Zakrzewski, V. G.; Dapprich, S.; Daniels, A. D.; Strain, M. C.; Farkas, O.; Malick, D. K.; Rabuck, A. D.; Raghavachari, K.; Foresman, J. B.; Ortiz, J. V.; Cui, Q.; Baboul, A. G.; Clifford, S.; Cioslowski, J.; Stefanov, B. B.; Liu, G.; Liashenko, A.; Piskorz, P.; Komaromi, I.; Martin, R. L.; Fox, D. J.; Keith, T.; Al-Laham, M. A.; Peng, C. Y.; Nanayakkara, A.; Challacombe, M.; Gill, P. M. W.; Johnson, B.; Chen, W.; Wong, M. W.; Gonzalez, C.; Pople, J. A. *Gaussian* 03, Revision C.02. Gaussian, Inc.: Wallingford CT, **2004**.
41. Scott, A. P.; Radom, L. Harmonic Vibrational Frequencies: An Evaluation of Hartree-Fock, Moller-Plesset, Quadratic Configuration Interaction, Density Functional Theory, and Semiempirical Scale Factors. *J. Phys. Chem.* **1996,** *100,* 16502–16513.
42. Bongiorno1, D.; Ceraulo1, L.; Lamartina1, L.; Natoli, M. C. Studies in Organic Mass Spectrometry. Part 25. Benzyl Ion Formation in Chemical Ionization (Methane or Isobutane) of Some *ortho* Alkylhetero-Substituted Diphenylcarbinols. *Rapid Commun. Mass Spectrom.* **2000,** *14,* 203–206.
43. Agozzino, P.; Ceraulo, L.; Ferrugia, M.; Lamartina, L. A New General Fragmentation Reaction in Mass Spectrometry. The Hydrogen–Carbon, Carbon–Carbon Double Rearrangement of 2-Heteroalkyl Substituted Diphenylmethyl Cations. *Eur. Mass Spectrom.* **1995,** *1,* 73–79.